Numerical Algorithms
https://doi.org/10.1007/s11075-025-02187-6

RESEARCH

Quaternion special least squares with Tikhonov regularization method in image restoration

Wenxiang Fei[1] · **Jia Tang**[1] · **Menghao Shan**[1]

Received: 18 April 2025 / Accepted: 23 July 2025

Abstract
In this paper, a color image restoration method based on Quaternion Special Least Squares with Tikhonov regularization method (QSLST) is proposed. In order to solve the problems of blur damage and noise degradation that may occur in the process of color image imaging, this method uses quaternion to represent the color image, and can consider the multi-channel spatial information of the image while processing the image restoration task. By introducing Tikhonov regularization term, the ill-conditioned problem in image restoration is effectively solved, and the stability and robustness of the restoration results are improved. The experimental results show that the proposed algorithm performs well in both quality and efficiency of color image restoration, and can effectively remove noise and blur in the image and recover clear image details.

Keywords Quaternion · QSLST · Tikhonov · Multi-channel · Image restoration

1 Introduction

With the development of digital image processing technology, image restoration has become crucial in medical imaging, remote sensing, etc. Yodjai et al. [35] proposed an example-based restoration method combining two-phase structural tensor and sparse representation, which effectively restores complex regions and provides a new idea for medical imaging. Jirakitpuwapat et al. [15] combined deep learning segmentation with example-based restoration which improves the restoration effect and is significant for remote sensing image restoration. The hybrid iterative scheme with variational inequalities by Abubakar et al. [1] provides a reference for image denoising and deblurring. The Halpern approximation method of Yodjai et al. [34] provides an optimization

Jia Tang contributed equally to this work.

✉ Jia Tang
tang_jia@126.com

[1] School of Mathematics and Statistics, Key Laboratory of Analytical Mathematics and Applications (Ministry of Education), Fujian Normal University, Fuzhou, Fujian 350117, People's Republic of China

Published online: 29 July 2025

scheme for image restoration under convex constraints. These researches promote the development of image restoration techniques and meet the practical needs in various fields.

In recent years, image restoration techniques have made significant progress in the field of artificial intelligence, mainly due to the innovative applications of transformer-based architectures, diffusion models and hybrid methods. Transformer-based architectures, such as Decomformer proposed by Lee et al. enhance the efficiency of image restoration by decomposing the self-attention mechanism [17]; Dou et al. combine RGB images with a transformer to provide a new idea for coded aperture snapshot spectral imaging restoration [7]. The diffusion model, on the other hand, generates high-quality images through gradual denoising, which is utilized by Zhong et al. to recover the tile patterns of ancient Chinese buildings, demonstrating strong texture restoration capabilities [40]. Hybrid methods, such as the regularization method that fuses the full variance and depth denoising prior proposed by Liang et al. [19], and the combination of depth image prior and sparse representation proposed by Xu et al. [31], both improve the robustness and detail preservation ability of restoration. Each of these methods has its own advantages, and future research will focus on their integration and innovation to address more complex image restoration challenges.

The traditional method faces the challenge of computational efficiency and numerical stability when dealing with large-scale pathological problems. To this end,researchers have proposed a variety of numerical algorithms to solve these problems. Saad and Schultz [23] proposed the generalized minimum residual algorithm(GMRES),and Paige and Saunders [21, 22] proposed the LSQR algorithm for solving sparse linear equations and least squares problems. These algorithms have been widely used in image restoration. For example, Xu et al. [30] applied the LSMR algorithm to image deblurring and achieved remarkable results. The GMRES algorithm is particularly effective in solving large-scale nonsymmetric linear systems,while the LSQR algorithm is well-suited for solving sparse linear equations and least squares problems. These methods have significantly contributed to the field of image restoration by providing efficient solutions to the underlying mathematical problems.

In recent years,matrix methods based on quaternions have received much attention for their high efficiency and robustness in processing color image and video data. Jia et al. [14] propose a robust quaternion matrix completion method for image restoration and show its advantages when dealing with large scale data. Similarly,Jia et al. [13] proposed a non-locally robust quaternion matrix completion method for large-scale color image and video restoration,further advancing the field. The Special least squares solutions of the quaternion matrix equation proposed by Zhang et al. [37] provide an important reference for image restoration. Quaternions offer a powerful mathematical framework for representing and manipulating color images and videos. By leveraging the unique properties of quaternions,these methods can efficiently handle the complex relationships between color channels,leading to improved restoration performance.

To overcome these challenges,the Tikhonov regularization method has been widely adopted due to its advantages in terms of stability and computational efficiency. Bouhamidi et al. [3, 4] proposed a conditional gradient method based on Tikhonov regularization and a Sylvester-Tikhonov regularization method for image restoration. Wang et al. [27] further combined the conjugate gradient least squares method to

propose a Tikhonov regularization method for large-scale ill-conditioned problems. These studies show that the Tikhonov regularization method has good robustness and convergence when dealing with pathological problems. Tikhonov regularization is particularly effective in stabilizing the solution process and improving the numerical stability of the algorithms. By adding a regularization term to the objective function,it helps to prevent overfitting and ensures that the solution is well-behaved,even in the presence of noise or incomplete data.

At the same time,image restoration methods based on diffusion models and nonlinear reaction-diffusion frameworks have also made remarkable progress. Garber and Tirer [11] proposed an image restoration method based on the denoising diffusion model,and Chen and Pock [5] proposed a trainable nonlinear reactive-diffusion framework for fast and effective image restoration. These methods significantly improve the performance of image recovery by introducing deep learning techniques. However,the existing methods still face the challenges of computational complexity and numerical stability when dealing with large-scale ill-conditioned problems. Diffusion-based methods leverage the principles of heat diffusion to propagate information across the image,effectively removing noise and artifacts. Nonlinear reaction-diffusion frameworks further enhance this process by incorporating adaptive mechanisms that respond to the local image structure. While these methods have shown great promise,they still need to address the challenges of scalability and robustness in practical applications.

Therefore, we propose an image restoration algorithm (QSLST) that combines quaternion special least squares and improved Tikhonov regularization. The difference between our algorithm and that of Jia et al. [13, 14] is that Jia et al. focus on the problem of color image complementation, while our algorithm focuses on the problem of denoising and deblurring image recovery from noisy images. This method has achieved a significant improvement over traditional technologies both theoretically and technically, mainly reflected in the following three aspects:

Firstly, inspired by two related papers [6, 37], this paper proposes a QSLST method for solving the image deblurring recovery problem. The method focuses on the least-paradigm least-squares solution of the quaternion matrix equation. However, unlike previous methods proposed in the literature, we note that the original method has some limitations in dealing with noisy images. In order to solve this problem, we innovatively introduce the Tikhonov regularization term into the QSLST method, which enables the method to have both denoising and deblurring capabilities. Through this improvement, the application scope of QSLST method is significantly expanded and its functions are more diversified, which can more effectively deal with complex image processing scenarios, especially when dealing with noise-contaminated blurred images, showing superior performance and wider application prospects.

Secondly, based on the isomorphic property of quaternion algebra, we have developed a special least squares framework with analytical solutions. This framework breaks through the bottleneck that the traditional quaternion matrix calculation relies on iterative solution, significantly improves the computational efficiency, and provides a more efficient solution path for the image restoration task.

Thirdly, the QSLST method introduces an adaptive regularization weight mechanism. While maintaining the stability of Tikhonov's regularization theory, this mechanism can adaptively suppress noise according to the spatial characteristics of

the image, thereby achieving more accurate image restoration in complex scenes. On the basis of maintaining the correlation between channels of color images, the QSLST method significantly improves the convergence speed of the algorithm through the analytical solution path of the special structure of quaternions. Meanwhile, by introducing the regularization term based on the quaternion F-norm, this method significantly improves the quality of image restoration while ensuring numerical stability.

Fourth, the main difference between the QSLST method and the latest related algorithms (e.g., GRL network, semi-supervised learning framework, diffusion model combined with Transformer's method) lies in its mathematical model-based nature. QSLST performs image deblurring and denoising through quaternionic matrix equations and Tikhonov regularization terms, with less dependence on training data and less computational resource requirements, and is suitable for real-time demanding scenarios with limited computing resources. , which is suitable for scenarios with high real-time requirements and limited computational resources. In contrast, although deep learning methods have advantages in complex image feature extraction, they usually require a large amount of data and computational resources for training and may not be flexible enough to deal with specific types of noise.

Finally, compared with the traditional quaternion-based image restoration algorithms, QSLST methods are more advantageous in dealing with noisy images. While the traditional methods are mainly applicable to images without noise or with less noise, QSLST is able to deal with image deblurring and denoising at the same time by introducing the Tikhonov regularization term, which extends the range of applications. In addition, the QSLST method is more efficient in constructing and solving mathematical models, which can better preserve image details and color features, and improve the stability and robustness of the restoration effect.

The experimental results show that the QSLST algorithm exhibits better noise-containing image restoration ability and structural similarity index when dealing with scenes such as blurring changes and noise pollution. The method provides a theoretical framework and implementation path for color image restoration in complex scenes, which has applicability and research value.

The remainder of this paper is organized as follows: In Section 2, we introduce the basic knowledge of quaternions and some quaternion operators. In Section 3, we consider tikhonov regularized image restoration model in matrix equation form. In Section 4, we introduce the Computational Complexity Analysis of the Moore-Penrose pseudo-inverse. In Section 5, we propose the QSLST algorithm for solving image recovery problem. In Section 6, We introduce adaptive parameters to obtain adaptive QSLST algorithm (AQSLST). The image restoration and comparison experiments are presented in Section 7. Finally, conclusions are drawn in Section 8.

2 Preliminaries

The quaternion set of numbers, which we denote by $\mathbb{H}$, is the skew field generated by the basis, satisfying the relation

$$i^2 = j^2 = k^2 = -1, \quad ij = -ji = k. \tag{1}$$

Any quaternion $q \in \mathbb{H}$ can be uniquely represented in the form

$$q = q_0 + q_1 i + q_2 j + q_3 k. \tag{2}$$

The conjugate and modulus of any quaternion $q = q_0 + q_1 i + q_2 j + q_3 k$ are defined as follows:

$$\overline{q} = q_0 - q_1 i - q_2 j - q_3 k, \tag{3}$$

$$\|q\| = \sqrt{\overline{q}q} = \sqrt{q_0^2 + q_1^2 + q_2^2 + q_3^2}. \tag{4}$$

If $q \in \mathbb{H}$ is non-zero, q^{-1} is defined as

$$q^{-1} = \frac{\overline{q}}{\|q\|^2}. \tag{5}$$

Next, we define two types of quaternion operators $\mathcal{A}$ and $\mathcal{U}$. For any quaternion matrix $Q = Q_0 + Q_1 i + Q_2 j + Q_3 k \in \mathbb{H}^{m\times n}$,

$$\mathcal{A}(Q) = \begin{pmatrix} Q_0 & -Q_1 & -Q_2 & -Q_3 \\ Q_1 & Q_0 & -Q_3 & Q_2 \\ Q_2 & Q_3 & Q_0 & -Q_1 \\ Q_3 & -Q_2 & Q_1 & Q_0 \end{pmatrix} \in \mathbb{R}^{4m\times 4n}. \tag{6}$$

For any quaternion vector $Q = Q_0 + Q_1 i + Q_2 j + Q_3 k \in \mathbb{H}^{m\times n}$,

$$\mathcal{U}(Q) = \begin{pmatrix} Q_0 \\ Q_1 \\ Q_2 \\ Q_3 \end{pmatrix} \in \mathbb{R}^{4m\times n}. \tag{7}$$

3 Image restoration model

Consider an image restoration problem, introducing the matrix equation

$$AX = B$$

where $A \in \mathbb{R}^{m\times n}$ is the blurring matrix representing the degradation process, and $X \in \mathbb{H}^{n\times p}$ is the original image matrix to be restored. $B \in \mathbb{H}^{m\times p}$ is the observed blurred image matrix.

Due to the discrete ill-posedness of the problem, the system $AX = B$ is typically unstable and does not have a unique solution. To address this, the problem is converted into a least squares problem:

$$\|AX - B\|_F^2 \to \min$$

This minimizes the Frobenius norm of the residual error between the restored image AX and the observed image B.

Additionally, due to noise interference, the observed image B can be expressed as:

$$B = \tilde{B} + n$$

where $\tilde{B}$ is the true but unobserved blurred image, and n represents additive noise. The noise n introduces instability in the least squares solution, necessitating regularization.

Introduce Tikhonov regularization in matrix form:

$$\left(\|AX - B\|_F^2 + \lambda\|X\|_F^2\right) \to \min$$

Here, the regularization term $\lambda\|X\|_F^2$ penalizes large magnitudes in the restored image X, where $\lambda > 0$ is the regularization parameter. This stabilizes the solution by balancing the trade-off between fidelity to the data B and smoothness of X.

Taking the derivative of the problem with respect to X, we get:

$$2A^H(AX - B) + 2\lambda X = 0$$

Here, A^H denotes the conjugate transpose of A.

Simplifying this gives the normal equation for the regularized least squares problem:

$$A^H AX + \lambda X = A^H B$$

This can be written as:

$$(A^H A + \lambda I)X = A^H B$$

where I is the identity matrix. The term $A^H A + \lambda I$ ensures that the matrix is invertible, even if $A^H A$ is rank-deficient or ill-conditioned.

Using the special minimal norm least squares solution for matrix equations, the solution X is given by:

$$X = (A^H A + \lambda I)^{\dagger} A^H B$$

where $(A^H A + \lambda I)^{\dagger}$ denotes the Moore-Penrose pseudo-inverse of $A^H A + \lambda I$. The pseudo-inverse provides the minimal Frobenius norm solution to the regularized problem.

The resulting X is the restored image. This approach effectively balances the trade-off between minimizing the residual error and suppressing noise amplification, leading to a stable and meaningful restoration of the original image.

4 The computational complexity analysis of the Moore-Penrose pseudo-inverse

The four-step process for calculating the Moor-Penrose pseudo-inverse of the given matrix A is as follows:

Singular Value Decomposition (SVD) To compute the Singular Value Decomposition (SVD) of a matrix $A \in \mathbb{R}^{m\times n}$(Suppose $m > n$), follow these steps:

Compute $A^T A$ and AA^T

- Compute $A^T A$:

$$A^T A = \begin{pmatrix} a_{11} & a_{21} & \cdots & a_{m1} \\ a_{12} & a_{22} & \cdots & a_{m2} \\ \vdots & \vdots & \ddots & \vdots \\ a_{1n} & a_{2n} & \cdots & a_{mn} \end{pmatrix} \begin{pmatrix} a_{11} & a_{12} & \cdots & a_{1n} \\ a_{21} & a_{22} & \cdots & a_{2n} \\ \vdots & \vdots & \ddots & \vdots \\ a_{m1} & a_{m2} & \cdots & a_{mn} \end{pmatrix}$$

  This results in an $n \times n$ square matrix $A^T A$.
- Compute AA^T:

$$AA^T = \begin{pmatrix} a_{11} & a_{12} & \cdots & a_{1n} \\ a_{21} & a_{22} & \cdots & a_{2n} \\ \vdots & \vdots & \ddots & \vdots \\ a_{m1} & a_{m2} & \cdots & a_{mn} \end{pmatrix} \begin{pmatrix} a_{11} & a_{21} & \cdots & a_{m1} \\ a_{12} & a_{22} & \cdots & a_{m2} \\ \vdots & \vdots & \ddots & \vdots \\ a_{1n} & a_{2n} & \cdots & a_{mn} \end{pmatrix}$$

  This results in an $m \times m$ square matrix AA^T.

Eigenvalue Decomposition of $A^T A$ and AA^T

- For $A^T A$:

$$A^T A\mathbf{v}_i = \lambda_i \mathbf{v}_i$$

  where λ_i are the eigenvalues and $\mathbf{v}_i$ are the eigenvectors. The matrix V is formed by the eigenvectors:

$$V = [\mathbf{v}_1, \mathbf{v}_2, \ldots, \mathbf{v}_n]$$

  The columns of V are the right singular vectors of A.
- For AA^T:

$$AA^T\mathbf{u}_i = \lambda_i \mathbf{u}_i$$

  where λ_i are the eigenvalues and $\mathbf{u}_i$ are the eigenvectors. The matrix U is formed by the eigenvectors:

$$U = [\mathbf{u}_1, \mathbf{u}_2, \ldots, \mathbf{u}_m]$$

  The columns of U are the left singular vectors of A.

Compute the Singular Values

- The singular values σ_i are the square roots of the eigenvalues λ_i:

$$\sigma_i = \sqrt{\lambda_i}$$

- The singular values are arranged in a diagonal matrix Σ:

$$\Sigma = \begin{pmatrix} \sigma_1 & 0 & \cdots & 0 \\ 0 & \sigma_2 & \cdots & 0 \\ \vdots & \vdots & \ddots & \vdots \\ 0 & 0 & \cdots & \sigma_{\min(m,n)} \end{pmatrix}$$

Form the SVD

- The SVD of A is given by:

$$A = U \Sigma V^T$$

Singular value processing In this step, we select the top k singular values of matrix A, where the magnitude of k is determined by default tolerance(The expression of default tolerance can be found in the pseudo-code flowchart 1). This means we retain only the largest k singular values and set the rest to zero. The processed diagonal matrix Σ' is given by:

$$\Sigma' = \begin{cases} \text{diag}(\sigma_1, \sigma_2, \ldots, \sigma_k, 0, \ldots, 0) & \text{if } k < \min(m, n) \\ \text{diag}(\sigma_1, \sigma_2, \ldots, \sigma_{\min(m,n)}) & \text{if } k = \min(m, n) \end{cases}$$

Matrix truncation Truncating the SVD involves retaining only the top k singular values and their corresponding singular vectors. This results in a low-rank approximation of the original matrix. The truncated SVD is given by:

$$A_k = U_k \Sigma_k V_k^T$$

where $U_k \in \mathbb{R}^{m \times k}$, $\Sigma_k \in \mathbb{R}^{k \times k}$, and $V_k \in \mathbb{R}^{n \times k}$.

Pseudo-inverse matrix calculation The pseudo-inverse of matrix A can be computed using the SVD. It is particularly useful for solving least squares problems. The pseudo-inverse $A^\dagger$ is defined as:

$$A^\dagger = V_k \Sigma_k^\dagger U_k^T$$

where $\Sigma_k^\dagger$ is the pseudo-inverse of Σ_k, obtained by taking the reciprocal of the non-zero singular values and transposing the matrix:

$$\Sigma_k^\dagger = \text{diag}\left(\frac{1}{\sigma_1}, \frac{1}{\sigma_2}, \ldots, \frac{1}{\sigma_k}\right)$$

The following is a pseudo-code diagram of the algorithm for solving the Moore-Penrose pseudo-inverse.

Algorithm 1 Algorithm for Computing the Moore-Penrose Pseudo-inverse of Matrix A

Input: Matrix A and tolerance tol
Output: Pseudo-inverse matrix X
Perform economy-size SVD on matrix A: $[U, S, V] = \text{svd}(A, \text{'econ'})$
Extract singular values: $s = \text{diag}(S)$
if tol is not specified **then**
    Compute default tolerance: $\text{tol} = \max(\text{size}(A)) \times \epsilon(\|s\|_\infty)$
end if
Count the number of singular values greater than tol: $r = \sum(s > \text{tol})$
Truncate matrices U and V and singular value array s:
$U = U(:, 1:r)$
$V = V(:, 1:r)$
$s = s(1:r)$
Compute the reciprocal of the singular values: $s_{\text{inv}} = 1./s$
Compute the pseudo-inverse matrix: $X = (V \cdot s_{\text{inv}}^{r}) \cdot U'$
Return X

Table 1 shows the computational complexity analysis of the algorithm.The next element is the calculation analysis. **Singular Value Decomposition (SVD)**: The selected Moor-Penrose pseudo-inverse algorithm performs an economy - size singular value decomposition of matrix A, which is the key step in computing the pseudo-inverse. The computational cost of SVD is relatively high. For an m n matrix A, assuming m n and n is the smaller dimension, its computational complexity is approximately $O(m^2n)$. **Singular Value Processing**: The step of extracting singular values and processing those below a given threshold is relatively simple. It mainly involves traversing the list of singular values and performing comparison and truncation operations, with a computational complexity of $O(k)$. **Matrix Truncation**: Based on the results of singular value processing, the columns of matrices U and V are truncated. The computational complexity of this operation is $O(mk+nk)$, but compared to SVD, the computational cost is relatively low. **Pseudo-inverse Matrix Calculation**: The Pseudo-inverse matrix is calculated using the truncated V, reciprocal of singular values, and the transpose of U. The computational complexity of this part mainly comes from matrix multiplication. Assuming the sizes of the truncated U and V are m r and n r respectively, the computational complexity is approximately $O(mk^2 + mkn)$.

Based on the above analysis, we can know that the computational complexity of the pseudo-inverse of matrix A is approximately $O(m^2n)$.

Table 1 Computational Complexity Analysis of Pseudo-inverse Calculation

Step	Time Complexity
Singular Value Decomposition (SVD)	$O(m^2n)$
Singular Value Processing	$O(k)$
Matrix Truncation	$O(mk+nk)$
Pseudo-inverse Matrix Calculation	$O(mk^2+mkn)$

5 QSLST algorithm

The transition from quaternion matrix to real matrix

To convert a quaternion matrix $A \in \mathbb{H}^{m\times n}$ into its real matrix, we can follow these steps:

Consider a quaternion matrix $A \in \mathbb{H}^{m\times n}$, where each element A can be represented as $A = A_0 + A_1 i + A_2 j + A_3 k$, with $A_0, A_1, A_2, A_3 \in \mathbb{R}^{m\times n}$.

Quaternion matrix A can be mapped to a $4m \times 4n$ real matrix representation:

$$A_r = \begin{bmatrix} A_0 & -A_1 & -A_2 & -A_3 \\ A_1 & A_0 & -A_3 & A_2 \\ A_2 & A_3 & A_0 & -A_1 \\ A_3 & -A_2 & A_1 & A_0 \end{bmatrix}$$

Considering the $\mathcal{A}$ operator mentioned in Section 2, we can obtain: $A_r = \mathcal{A}(\mathrm{A})$.

Next, we select the first column block of matrix A_r.

$$A_r^c = \begin{bmatrix} A_0 \\ A_1 \\ A_2 \\ A_3 \end{bmatrix}$$

Considering the $\mathcal{U}$ operator mentioned in Section 2, we can obtain: $A_r^c = \mathcal{U}(\mathrm{A})$.

The two theorems given below indicate that we can solve the image restoration model 3 presented above through the least norm least squares solution.

Theorem 1 *Let $T \in \mathbb{H}^{m\times n}$ and $E \in \mathbb{H}^{m\times p}$ such that $T = A^H A + \lambda I$ and $E = A^H B$. Then the set $S_{\mathbb{H}}$ of Image restoration model can be expressed as:*

$$S_{\mathbb{H}} = \left\{ X \in \mathbb{H}^{n\times p} \mid \mathcal{U}(X) = \mathcal{A}(T)^{\dagger}\mathcal{U}(E) + \left(I_{4n} - \mathcal{A}(T)^{\dagger}\mathcal{A}(T)\right) Y,\ \forall Y \in \mathbb{R}^{4n\times p} \right\},$$

where $Y \in \mathbb{R}^{4n\times p}$ is an arbitrary matrix. Furthermore, the minimal norm least squares solution $X_{\mathbb{H}} \in S_{\mathbb{H}}$ satisfies:

$$\mathcal{U}(X_{\mathbb{H}}) = \mathcal{A}(T)^{\dagger}\mathcal{U}(E).$$

Proof According to Preliminaries, the Frobenius norm of $TX - E$ can be expressed as:

$$\|TX - E\|_F = \|\mathcal{U}(TX - E)\|_F = \|\mathcal{A}(T)\mathcal{U}(X) - \mathcal{U}(E)\|_F .$$

Thus, the problem of minimizing $\|TX - E\|_F$ is equivalent to minimizing $\|\mathcal{A}(T)\mathcal{U}(X) - \mathcal{U}(E)\|_F$.

For the real matrix equation $TX = E$, according to Wei [28] the least squares solutions can be represented as:

$$\mathcal{U}(X) = \mathcal{A}(T)^{\dagger}\mathcal{U}(E) + \left(I_{4n} - \mathcal{A}(T)^{\dagger}\mathcal{A}(T)\right) Y, \quad \forall Y \in \mathbb{R}^{4n\times p}.$$

Here, $\mathcal{A}(T)^{\dagger}$ denotes the Moore-Penrose inverse of $\mathcal{A}(T)$, and I_{4n} is the identity matrix of size $4n \times 4n$.

The minimal norm least squares solution $X_{\mathbb{H}} \in S_{\mathbb{H}}$ is obtained by setting $Y = 0$, which gives:

$$\mathcal{U}(X) = \mathcal{A}(T)^{\dagger}\mathcal{U}(E).$$

This completes the proof. □

Theorem 2 *Let $T \in \mathbb{H}^{m\times n}$ and $E \in \mathbb{H}^{m\times p}$ such that $T = A^H A + \lambda I$ and $E = A^H B$. The equation $TX = E$ has a solution $X \in \mathbb{H}^{n\times p}$ if and only if:*

$$I_{4n} - \mathcal{A}(T)^{\dagger}\mathcal{A}(T) = 0.$$

Proof From Theorem 1, we have:

$$\|TX - E\|_F = \|\mathcal{A}(T)\mathcal{U}(X) - \mathcal{U}(E)\|_F .$$

The equation $TX = E$ has a solution if and only if $\|TX - E\|_F = 0$. This implies:

$$\|\mathcal{A}(T)\mathcal{U}(X) - \mathcal{U}(E)\|_F = 0.$$

And that immediately solves the following equation:

$$\left\|\mathcal{A}(T)\mathcal{A}(T)^{\dagger}\mathcal{A}(T)\mathcal{U}(X) - \mathcal{U}(E)\right\|_F = 0.$$

Substituting $\mathcal{U}(E) = \mathcal{A}(T)\mathcal{U}(X)$ into the above equation, we get:

$$\left\|\left(\mathcal{A}(T)\mathcal{A}(T)^{\dagger} - I_{4n}\right)\mathcal{U}(E)\right\|_F = 0.$$

This is equivalent to:

$$\left((\mathcal{A}(T)\mathcal{A}(T)^{\dagger} - I_{4n}\right)\mathcal{U}(E) = 0.$$

Thus, the equation $TX = E$ has a solution if and only if the above condition holds. □

The following content will analyze the computational complexity of $\mathcal{A}(T)^{\dagger}$:

To analyze the computational complexity of solving $\mathcal{A}(T)^{\dagger}$, we start by noting that $\mathcal{A}(T)$ is a $4m \times 4n$ matrix. The pseudo-inverse computation, as discussed in Section 4, involves several key steps whose complexities must be considered:(The k mentioned below is the rank of $\mathcal{A}(T)$)

- **Singular Value Decomposition (SVD)**: The pseudo-inverse $\mathcal{A}(T)^{\dagger}$ is typically computed via SVD, which decomposes $\mathcal{A}(T)$ into $U\Sigma V^T$. For a $4m \times 4n$ matrix, the SVD complexity is dominated by the cost of reducing the matrix to bidiagonal form and then computing the SVD of the bidiagonal matrix. This process has a complexity of approximately $O(16mn \cdot \max(4m, 4n))$.

- **Matrix Truncation**: Once the singular values are obtained, the columns of matrices U and V are truncated. The computational complexity of this operation is $O(4mk + 4nk)$.
- **Pseudo-inverse Matrix Calculation**: The final step involves matrix calculation to form $\mathcal{A}(T)^{\dagger} = V_k \Sigma_k^{+} U_k^{T}$. Multiplying two matrices of appropriate dimensions has a complexity that depends on the exact dimensions and multiplication order. For the given matrix dimensions, this step also increases the overall complexity($O(4mk^2 + 16mkn)$).

Combining these steps, the dominant term in the complexity analysis for computing the pseudo-inverse of a $4m \times 4n$ matrix is found to be $O(16mn \cdot \max(4m, 4n))$, as detailed in Section 4. Then we can obtain the result of the main computational complexity in the calculation of $\mathcal{A}(T)^{\dagger}$ as follows: (Suppose $m > n$)

$$\text{Computational Complexity of } \mathcal{A}(T)^{\dagger} = O(64m^2 n) \tag{8}$$

The following content considers algorithms, The QSLST algorithm is designed to restore damaged images affected by blurring and noise. It leverages quaternion algebra to represent color images and combines least squares optimization with Tikhonov regularization to achieve robust image recovery. Below is a detailed description of the algorithm:

Algorithm 2 Quaternion Special Least Squares with Tikhonov Regularization (QSLST) for Image Restoration

1: **Input:** Damaged image (blurring operator and noise) converted into quaternion matrix $X \in \mathbb{H}^{n \times p}$, parameters $A \in \mathbb{R}^{m \times n}$, $B \in \mathbb{H}^{m \times p}$, λ.

2: Convert the problem into a least squares problem:

$$\|AX - B\|_F^2 \to \min .$$

3: Introduce Tikhonov regularization:

$$\left(\|AX - B\|_F^2 + \lambda \|X\|_F^2\right) \to \min .$$

4: Take the derivative of the problem:

$$A^H AX + \lambda X = A^H B.$$

5: Let $T = A^H A + \lambda I$ and $E = A^H B$.

6: Use operators to rewrite the least squares problem:

$$\mathcal{A}(T)\mathcal{U}(X) = \mathcal{U}(E).$$

7: Solve for $\mathcal{U}(X)$:

$$\mathcal{U}(X) = \mathcal{A}(T)^{\dagger}\mathcal{U}(E).$$

8: Get restored image X:

$$X = \mathcal{U}^{-1}(X).$$

9: **Output:** Restored image X.

Problem formulation The QSLST algorithm begins by representing the damaged image as a quaternion matrix $X \in \mathbb{H}^{n\times p}$, where $\mathbb{H}$ denotes the quaternion algebra. This representation allows the algorithm to handle color images in a unified manner, avoiding the need to process each color channel separately. The blurring operator is represented by a real matrix $A \in \mathbb{R}^{m\times n}$, and the observed data is represented by a quaternion matrix $B \in \mathbb{H}^{m\times p}$.

The primary goal is to solve the least squares problem:

$$\|AX - B\|_F^2 \to \min,$$

where $\|\cdot\|_F$ denotes the Frobenius norm. This formulation aims to find a matrix X that minimizes the difference between the blurred image AX and the observed data B.

To address the ill-posed nature of the problem and prevent overfitting, Tikhonov regularization is introduced. The regularized problem becomes:

$$\left(\|AX - B\|_F^2 + \lambda\|X\|_F^2\right) \to \min,$$

where $\lambda > 0$ is a regularization parameter that balances the trade-off between data fidelity and solution smoothness. The regularization term $\lambda\|X\|_F^2$ ensures that the solution X is stable and well-conditioned, even in the presence of noise.

Taking the derivative of the regularized problem with respect to X, we obtain the following linear equation:

$$A^H AX + \lambda X = A^H B,$$

where A^H denotes the conjugate transpose of A. This equation can be rewritten as:

$$TX = E,$$

where $T = A^H A + \lambda I$ and $E = A^H B$.

To solve this equation efficiently, the algorithm uses quaternion operators $\mathcal{A}$ and $\mathcal{U}$ to transform the problem into:

$$\mathcal{A}(T)\mathcal{U}(X) = \mathcal{U}(E).$$

The solution for $\mathcal{U}(X)$ is obtained using the Moore-Penrose pseudo-inverse:

$$\mathcal{U}(X) = \mathcal{A}(T)^{\dagger}\mathcal{U}(E).$$

Finally, the restored image X is recovered by applying the inverse operator $\mathcal{U}^{-1}$.

The following are the advantages of the QSLST method:

- **Quaternion Representation** The use of quaternion algebra provides a unified framework for handling color images. Unlike traditional methods that process each color channel independently, QSLST treats the RGB components as a single quaternion entity. This approach preserves color correlations and avoids color distortion, resulting in more natural and accurate image restoration.
- **Stability and Robustness** Tikhonov regularization significantly enhances the stability of the solution. By incorporating the regularization term $\lambda\|X\|_F^2$, the algorithm effectively suppresses high-frequency noise and prevents overfitting. This makes QSLST particularly robust in scenarios with significant noise or ill-conditioned blurring operators.
- **Efficiency** The algorithm leverages the Moore-Penrose pseudo-inverse to solve the linear system directly, avoiding the need for iterative optimization. This direct approach ensures computational efficiency, even for large-scale image restoration problems. The use of quaternion operators further simplifies the computation, making the algorithm suitable for real-time applications.
- **Mathematical Rigor** The algorithm is grounded in solid mathematical principles, combining linear algebra, quaternion theory, and optimization techniques. This rigorous foundation ensures that the solution is both theoretically sound and practically effective, providing reliable performance across diverse image restoration tasks.

6 AQSLST algorithm

Generalized Cross Validation (GCV) Algorithm

The Generalized Cross Validation (GCV) algorithm is a powerful data-driven method designed for selecting regularization parameters in inverse problems. This technique is widely used in various fields such as image processing, signal recovery, and statistical modeling, where the goal is to balance the trade-off between the goodness of fit and the complexity of the model. The primary objective of GCV is to minimize the prediction error by adaptively determining the optimal regularization parameter without requiring prior knowledge of the noise level or the exact structure of the data. Unlike traditional cross-validation methods that rely on splitting the dataset into training and validation sets, GCV leverages the entire dataset to compute an unbiased estimate of the prediction error, making it computationally efficient and robust in scenarios with limited data.

The GCV algorithm is particularly advantageous in ill-posed inverse problems, where small perturbations in the input data can lead to significant deviations in the solution. By incorporating a regularization term, GCV ensures that the solution remains stable and generalizes well to unseen data. This adaptability makes GCV a versatile tool in applications such as image restoration, where the degradation process (e.g., blurring, noise) is often unknown or difficult to model explicitly.

The adaptive parameter selection via GCV involves the following detailed steps:

- **Compute the GCV Function for a Range of λ Values**: To find the optimal regularization parameter, GCV evaluates the function $G(\lambda)$ over a predefined range of λ values. This range is typically chosen based on prior knowledge or through an exploratory grid search. For each λ, the corresponding solution $X(\lambda)$ is computed by solving the regularized least squares problem:

$$X(\lambda) = (A^H A + \lambda I)^{-1} A^H B$$

  The GCV function $G(\lambda)$ is then evaluated using the computed $X(\lambda)$.
- **Find the Optimal λ^* by Minimizing** $G(\lambda)$: The optimal regularization parameter λ^* is determined by minimizing the GCV function over the range of λ values. This minimization can be performed using numerical optimization techniques such as golden section search or gradient descent. The choice of optimization algorithm depends on the computational complexity and the smoothness of the GCV function.
- **Use λ^* to Solve the Regularized Least Squares Problem**: Once the optimal λ^* is identified, it is used to compute the final solution $X(\lambda^*)$ by solving the regularized least squares problem. This solution balances the trade-off between fidelity to the observed data and smoothness, ensuring that the restored image is both visually plausible and statistically consistent with the input data.

The adaptive nature of GCV makes it particularly suitable for scenarios where the noise level or the degradation process is unknown. By systematically exploring the parameter space and selecting the λ that minimizes the prediction error, GCV provides a robust and automated approach to parameter selection.

Application in image restoration

In the context of image restoration, the GCV algorithm plays a critical role in adaptively selecting the regularization parameter λ for Tikhonov regularization. Tikhonov regularization is a widely used technique that adds a penalty term to the least squares objective function to enforce smoothness in the restored image. The regularized objective function is given by:

$$\min_X \|AX - B\|_F^2 + \lambda \|LX\|_F^2$$

where L is a regularization matrix (e.g., a discrete Laplacian operator) that enforces smoothness constraints on the solution X.(In this paper L takes the identity matrix.)

The GCV algorithm ensures that the restored image X is both smooth and faithful to the observed data B. By adaptively determining the optimal λ, GCV allows the restoration process to handle varying levels of noise and blurring without requiring prior knowledge of the noise characteristics or the exact degradation model. This adaptability is particularly valuable in practical applications where the degradation process (e.g., blurring kernel) is often unknown or difficult to estimate accurately.

Moreover, GCV provides a principled way to avoid over-smoothing or under-smoothing the restored image. Over-smoothing can lead to loss of fine details, while under-smoothing may result in residual noise or artifacts. By minimizing the GCV function, the algorithm automatically adjusts the regularization strength to achieve the optimal balance between these competing objectives.

In summary, the GCV algorithm is a versatile and robust method for parameter selection in image restoration and other inverse problems. Its ability to adaptively determine the regularization parameter without prior assumptions about the noise or degradation process makes it an indispensable tool in modern image processing and computer vision applications.

Additionally, selecting an appropriate regularization parameter λ is crucial, which can be achieved using the GCV method [12]. We now revisit the GCV method to ascertain the regularization parameter λ.

Consider the generalized singular value decomposition (GSVD) [26] of the matrix pair (A, L) $(A \in \mathbb{R}^{m\times n}, L \in \mathbb{R}^{m\times n})$. There exist orthogonal matrices U, V and a non-singular matrix N such that

$$U^T AN = \text{diag}(c_1, c_2, \cdots, c_n), \tag{9}$$

$$V^T LN = \text{diag}(s_1, s_2, \cdots, s_n), \tag{10}$$

where $\{c_i\}_{i=1}^n$ and $\{s_i\}_{i=1}^n$ are the positive generalized singular values of A and L respectively. Consequently, the value of the regularization parameter λ is determined by minimizing the GCV function

$$\text{GCV}(\lambda) = \frac{\sum_{i=1}^{n} \left(\frac{s_i^2 \tilde{g}_i}{c_i^2 + \lambda^2 s_i^2} \right)^2}{\left(\sum_{i=1}^{n} \frac{s_i^2}{c_i^2 + \lambda^2 s_i^2} \right)^2}, \tag{11}$$

where $\tilde{g} = U^T g$.

Considering that the AQSLST algorithm is also to solve the pseudo-inverse of $\mathcal{A}(T)^\dagger$, its computational complexity is the same as that of the QSLST algorithm (see Section 4, Section 5).

The built-in GCV function will traverse the value range of the set parameter λ_2 and index the abscissa of the minimum value point of the function. The abscissa is the selected optimal parameter λ_2.As shown in the following figure:

The pseudo-code flowchart of the AQSLST algorithm is as follows:

Algorithm 3 Adaptive Quaternion Special Least Squares with Tikhonov regularization (AQSLST) for Image Restoration

1: **Input:** Damaged image (blurring operator and noise) converted into quaternion matrix $X \in \mathbb{H}^{n\times p}$, parameters $A \in \mathbb{R}^{m\times n}$, $B \in \mathbb{H}^{m\times p}$.
2: Convert the problem into a least squares problem:

$$\|AX - B\|_F^2 \to \min .$$

3: Introduce Tikhonov regularization with adaptive parameter λ:

$$\left(\|AX - B\|_F^2 + \lambda\|X\|_F^2\right) \to \min .$$

4: Take the derivative of the problem:

$$A^H AX + \lambda X = A^H B.$$

5: Let $T = A^H A + \lambda I$ and $E = A^H B$.
6: **Adaptive Parameter Selection via GCV:**
7: Compute the GCV function:

$$G(\lambda) = GCV(\lambda).$$

8: Find the optimal λ by minimizing $G(\lambda)$:

$$\lambda^* = \arg\min_{\lambda} G(\lambda).$$

9: Use operators to rewrite the least squares problem with $T^* = A^H A + \lambda^* I$:

$$\mathcal{A}(T^*)\mathcal{U}(X) = \mathcal{U}(E).$$

10: Solve for $\mathcal{U}(X)$:

$$\mathcal{U}(X) = \mathcal{A}(T^*)^{\dagger}\mathcal{U}(E).$$

11: Get restored image X:

$$X = \mathcal{U}^{-1}(X).$$

12: **Output:** Restored image X.

The introduction of the Generalized Cross-Validation (GCV) function in the Adaptive Quaternion Special Least Squares with Tikhonov regularization (AQSLST) algorithm provides several key advantages for image restoration (Fig. 1).

GCV function eliminates the need for manual tuning of the regularization parameter λ. By minimizing the GCV function $G(\lambda)$, the algorithm automatically selects the optimal λ^* that balances the trade-off between fitting the data and avoiding overfitting. This automation is particularly beneficial in scenarios where the noise level or blurring operator is unknown or varies across different images.

This criterion is designed to be robust to noise in the data. By incorporating the trace containing the regularization matrix $T^{-1}A^H$, the GCV function accounts for the complexity of the model and the influence of noise. This ensures that the selected λ^* is not overly sensitive to random fluctuations in the data, leading to more stable and reliable image restoration results. And the adaptive nature of the GCV function allows the algorithm to adjust λ based on the specific characteristics of the input image. For instance, if the image contains high levels of noise or severe blurring, the GCV function

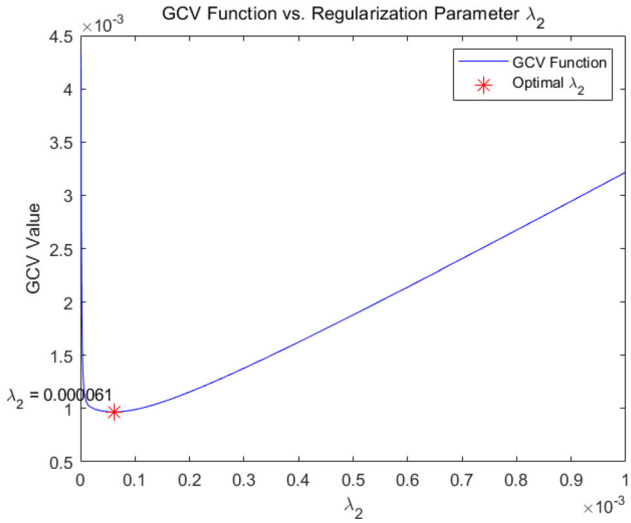

Fig. 1 The selection of the optimal parameters of λ_2 in the GCV function

will select a larger λ to enforce stronger regularization. Conversely, for cleaner or less blurred images, a smaller λ will be chosen, preserving more fine details.

Minimizing the GCV function provides a systematic and efficient way to optimize λ. Unlike grid search or other brute-force methods, the GCV criterion offers a continuous and differentiable objective function, allowing for faster convergence to the optimal parameter. This efficiency is critical for real-time or large-scale image restoration applications.

By selecting the optimal λ^*, the GCV function ensures that the restored image strikes the right balance between fidelity to the input data and smoothness. This results in higher quality restorations with reduced artifacts and better preservation of edges and textures.

The GCV function is not limited to Tikhonov regularization. It can be extended to other regularization terms, such as total variation or wavelet-based regularization, making the algorithm versatile for different image restoration tasks. And it avoids the need for cross-validation, which typically requires splitting the data into training and validation sets. Instead, it uses the entire dataset to compute the optimal λ, reducing computational overhead while maintaining robust performance.

7 Experiments

To illustrate the efficacy of the QSLST algorithm in solving the matrix system $AX = B$ and its application to image restoration, several numerical examples are presented. The numerical experiments were carried out using MATLAB R2018a on an Intel(R) Core(TM) i5-8300H CPU @ 2.30GHz, 8 GB RAM computer.

We employ a variety of commonly used standard test images as the original images X, such as "fruits,", "airplane,", "tulips,", "monarch," and "kodim11," as depicted in the figures. The QSLST method is compared with several other methods for image restoration testing within the framework of the reduced biquaternion algorithm. These methods include Algorithm 1 proposed by Yuan et al. [36], the CGLS method proposed by Michael Saunders et al., the LSMR method proposed by Fong and Saunders [10], and the LSQR method proposed by Paige and Saunders [21]. In order to ensure the balance, we implement all experimental methods under the quaternion image restoration model.

SSIM (Structural Similarity Index) is an index used to measure the visual similarity between two images, and its formula is as follows:

$$SSIM(x, y) = \frac{(2\mu_x\mu_y + c_1)(2\sigma_{xy} + c_2)}{(\mu_x^2 + \mu_y^2 + c_1)(\sigma_x^2 + \sigma_y^2 + c_2)}$$

where μ represents the mean, σ represents the standard deviation, σ_{xy} represents the covariance, and c_1, c_2 are small constants set to avoid having a zero denominator.

PSNR (Peak signal-to-noise ratio) is an important indicator of image quality, which is defined as:

$$PSNR = 10 \cdot \log_{10}\left(\frac{MAX_I^2}{MSE}\right)$$

where MAX_I is the maximum possible pixel value of the image and MSE is the mean square error

RE (Relative error) is a measure of the difference between the restored image and the original image, defined as:

$$RE(X) = \frac{\|X - X^*\|_F}{\|X^*\|_F}$$

where X is the recovered image and X^* is the original image, representing the Frobenius norm.

The Gaussian Noise SNR of the following experiments is 30 dB and in 7.6 Example 5, we consider the quality of image restoration in four Gaussian Noise SNR of 15, 20, 25, and 30. The values of the selected parameter in the experiment below are chosen as 0.0005 according to the sensitivity analysis 7.1, and the range of λ values tested is from 10^{-6} to 10^{-3}.

7.1 Sensitivity analysis

In the field of image restoration, selecting an appropriate regularization parameter λ_2 for Tikhonov regularization is crucial for achieving optimal image recovery. Using the "airplane" image as an example, we conduct a sensitivity analysis to determine the critical value of λ_2.

We define $\Delta X = X(\lambda_2+\Delta\lambda_2)-X(\lambda_2)$, where $X(\lambda_2)$ represents the restored image with the regularization parameter λ_2. The sensitivity of λ_2 is evaluated by considering both the Frobenius norm of ΔX and the PSNR of the restored image.

Initially, we set λ_2 to a relatively large value of 0.5 and use a perturbation of 0.1. As we iteratively reduce λ_2, we observe the Frobenius norm of ΔX and the PSNR of the restored image. When the Frobenius norm of ΔX continues to decrease and the PSNR improves significantly, it indicates that λ_2 is sensitive and needs further adjustment. We continue to decrease λ_2 to 0.05 with a smaller perturbation of 0.01, and repeat this process.

The repeated process is as follows:

- Start with $\lambda_2 = 0.5$ and $\Delta\lambda_2 = 0.1$.
- Compute $\Delta X = X(\lambda_2 + \Delta\lambda_2) - X(\lambda_2)$.
- Calculate the Frobenius norm of ΔX and the PSNR of the restored image.
- If the Frobenius norm of ΔX decreases and the PSNR improves, reduce λ_2 to $0.1\lambda_2$.
- Adjust $\Delta\lambda_2$ as needed (e.g., reduce it to 0.01 when λ_2 reaches 0.05).
- Repeat steps 2-5 until the Frobenius norm of ΔX begins to increase and the improvement in PSNR becomes insignificant.

Eventually, when the Frobenius norm of ΔX starts to increase and the PSNR improvement is no longer significant, we consider this point as the critical value for λ_2, which is determined to be 0.0005 in this case. This critical value of $\lambda_2 = 0.0005$ is then used as the selected regularization parameter in our experiments.

7.2 Example 1

In Example 1, we perform Gaussian blur and Gaussian noise processing on the image. First of all, we define the parameters of the Gaussian function, including the standard deviation of the Gaussian blur kernel and the blur radius. After this, create the Toeplitz matrix H and use it as the image matrix to downgrade the original image. During the image acquisition process, due to factors such as insufficient lighting, uneven brightness, interference from circuit components, and long-term high-temperature operation of the sensor, the image sensor will generate Gaussian noise. In addition, due to inaccurate camera focusing or motion blur, the image may become blurry. The combination of Gaussian blur and Gaussian noise effectively simulates the image distortion caused by sensor performance and shooting conditions.

And the point spread function is:

$$h(x, y) = \begin{cases} \frac{1}{2\pi\sigma^2} e^{-\frac{x^2+y^2}{2\sigma^2}}, & \text{if } |x - y| \le r \\ 0, & \text{otherwise} \end{cases}$$

Where σ is the standard deviation, controlling the degree of ambiguity.

The numerical results of Fig 2 are shown in Table 2 as follows. In Table 2, the QSLST method demonstrated outstanding performance and was significantly superior

Fig. 2 The blurred and noisy images with r=2,4 (left column) and their restored results(Starting from the second left, they are QSLST, Algorithm 1[23],CGLS, LSQR, and LSMR respectively)

to several other common image restoration algorithms. Specifically, when the parameter $r = 2$, the peak signal-to-noise ratio (PSNR) of the QSLST method reached 32.2966, which is the highest among all comparison methods, indicating its excellent performance in restoring the details of the image and reducing noise. Meanwhile, its Structural Similarity Index Measure (SSIM) value is 0.9745, close to 1, meaning that the restored image is highly consistent with the original image in terms of structure and texture, and the visual effect is very close. The relative error (RE) is only 0.0298, indicating that the difference between the restored image and the original image is extremely small and can almost be ignored. Even in the case of the parameter $r = 4$, the QSLST method still maintains excellent performance. Its PSNR is 26.957, SSIM is 0.9131, and RE is 0.0585. These indicators are still the best among all methods. This indicates that the QSLST method can effectively restore the image quality under different parameter Settings, especially when $r = 2$, its restoration effect is the most significant, which can restore the original features and details of the image to the greatest extent. For the image restoration task, the QSLST method is undoubtedly a very reliable choice.

Table 2 The PSNR, SSIM and RE of the restored images

Method	Parameter	PSNR	SSIM	RE
QSLST	$r = 2$	32.2966	0.9745	0.0298
	$r = 4$	26.957	0.9131	0.0585
Algorithm 1 [36]	$r = 2$	30.9269	0.9711	0.0376
	$r = 4$	25.639	0.9089	0.0597
CGLS	$r = 2$	31.2681	0.974	0.0335
	$r = 4$	26.2087	0.912	0.0619
LSQR	$r = 2$	27.4654	0.968	0.0476
	$r = 4$	22.9024	0.8642	0.086
LSMR	$r = 2$	29.351	0.9734	0.0455
	$r = 4$	23.6634	0.88	0.0797

7.3 Example 2

In Example 2, we processed the image with motion blur and Gaussian noise, and defined the direction and length of the motion blur. By creating the Toeplitz matrix H, whose first row represents, for example, the motion blur kernel, the image blur effect caused by camera shake or rapidly moving objects during the shooting process can be simulated. By adding Gaussian noise, the noise interference image in a specific environment is simulated. It is applicable to image restoration in dynamic scenes.

And the point spread function is:

$$h(x, y) = \begin{cases} \frac{1}{r}, & \text{if } x^2 + y^2 \leq r^2 \text{ and } \frac{y}{x} = \tan(\theta) \\ 0, & \text{otherwise} \end{cases}$$

Where r is the blurred scale and θ is the Angle between the direction of motion and the positive X-axis.

The numerical results of Fig. 3 are shown in Table 3 as follows. In Table 3, different image restoration methods were compared and analyzed when the degree of motion blur was 10 and 20. The results show that the QSLST method performs best in both degrees of ambiguity. When the motion blur is 10, the PSNR of QSLST is 28.1323, the SSIM is 0.9049, and the RE is 0.0338. When the motion blur is 20, its PSNR is 25.569, SSIM is 0.841, and RE is 0.0472. These indicators are the best among all methods. Furthermore, with the increase of the degree of blurriness, the PSNR and SSIM values of all methods decreased, while the RE value increased, indicating that the image restoration quality decreased with the intensification of the degree of blurriness. This indicates that in the image restoration task, the QSLST method can better deal with motion blur of different degrees, especially when the degree of blur is small, the restoration effect is more significant.

7.4 Example 3

To compare the adaptive AQSLST method and the QSLST method, we conducted image restoration tests using two common types of image degradation: Gaussian blur

Fig. 3 The blurred and noisy images with Horizontal=10,20 (left column) and their restored results(Starting from the second left, they are QSLST, Algorithm 1[23],CGLS, LSQR, and LSMR respectively)

Table 3 The PSNR, SSIM and RE of the restored images

Method	Parameter	PSNR	SSIM	RE
QSLST	Horizontal=10	28.1323	0.9049	0.0338
	Horizontal=20	25.569	0.841	0.0472
Algorithm 1 [36]	Horizontal=10	27.7104	0.9053	0.0377
	Horizontal=20	24.4273	0.8467	0.0468
CGLS	Horizontal=10	27.43	0.9028	0.0349
	Horizontal=20	24.4395	0.8406	0.0473
LSQR	Horizontal=10	26.7279	0.8948	0.0321
	Horizontal=20	22.5087	0.8571	0.0642
LSMR	Horizontal=10	26.9556	0.9023	0.028
	Horizontal=20	22.5739	0.8536	0.0554

and Gaussian noise. These two phenomena are often encountered in actual imaging scenarios, such as optical systems with limited resolution and sensor noise during image acquisition or transmission (For specific details, see Example 1).

The numerical results of Fig. 4 are shown in Table 4 as follows. In Table 4, the AQSLST method demonstrated significant superiority in the image restoration task

Fig. 4 The blurred and noisy images with r=1,2,3,4 (left column) and their restored results(From left to right are the blurred noisy image, the restored image by AQSLST, and the restored image by QSLST)

Table 4 The PSNR, SSIM and RE of the restored images

Method	Parameter	PSNR	SSIM	RE
AQSLST	$r = 1$	35.8686	0.9919	0.0254
	$r = 2$	33.2248	0.9917	0.0262
	$r = 3$	27.663	0.9502	0.0743
	$r = 4$	26.7222	0.9382	0.0904
QSLST	$r = 1$	34.2161	0.9896	0.0303
	$r = 2$	31.3906	0.9876	0.0362
	$r = 3$	27.0424	0.9513	0.0719
	$r = 4$	25.9618	0.932	0.0956

through an adaptive parameter adjustment mechanism. Compared with the QSLST method, AQSLST shows higher PSNR and SSIM values as well as lower RE values under different parameter r Settings. For example, when $r = 1$, the PSNR of AQSLST is as high as 35.8686, the SSIM is 0.9919, and the RE is only 0.0254, while the PSNR of QSLST is 34.2161 and the SSIM is 0.9896. RE is 0.0303. Even when r increases, AQSLST can still maintain a better recovery effect. Especially when $r = 2$ and $r = 4$, its PSNR and SSIM values are both higher than those of QSLST, and the RE is lower at the same time. This indicates that the AQSLST method can automatically optimize the restoration effect according to different image characteristics and parameter Settings, effectively improve the quality of image restoration, reduce errors, and stably output high-quality restored images.

7.5 Example 4

To assess the performance of the adaptive AQSLST method relative to the conventional QSLST method, we constructed a detailed testing framework in Example 4, incorporating two prevalent image degradation elements: motion blur and uniform noise. The integration of these factors allows us to examine the extent to which the adaptive AQSLST method can handle motion blur and noise more effectively than the standard QSLST method, particularly with regard to edge preservation, clarity enhancement, and artifact reduction. (For more detailed information, refer to Example 2.)

The numerical results of Fig. 5 are shown in Table 5 as follows. In Table 5, the AQSLST method demonstrated significant superiority over the QSLST method. Under different motion blur parameters, the PSNR and SSIM values of the AQSLST method are higher, and the RE value is lower, indicating that the restored images have higher clarity, better structural similarity and lower error. For example, when the motion blur is 5, the PSNR of AQSLST reaches 31.2347, the SSIM is 0.9771, and the RE is only 0.0424, while the PSNR of QSLST is 29.5827, the SSIM is 0.9545, and the RE is 0.0471. As the degree of blur increases, AQSLST can still maintain a better recovery effect. Especially when the motion blur is 10, 15, and 20, all its indicators are superior to QSLST. This highlights the strong adaptability and robustness of the AQSLST method when dealing with different degrees of blurriness, and it can automatically adjust parameters to optimize the quality of image restoration.

Fig. 5 The blurred and noisy images with Horizontal=5,10,15,20 (left column) and their restored results(From left to right are the blurred noisy image, the restored image by AQSLST, and the restored image by QSLST)

7.6 Example 5

To evaluate the performance of the adaptive AQSLST method compared to the standard QSLST method, in Example 5, we constructed a test framework with different noise sizes (35dB, 30dB, 25dB, 20dB), which included two common image degradation elements: motion blur(Horizontal=10) and Gaussian noise. The integration of these factors enables us to examine the extent to which the adaptive AQSLST method handles

Table 5 The PSNR, SSIM and RE of the restored images

Method	Parameter	PSNR	SSIM	RE
AQSLST	Horizontal=5	31.2347	0.9771	0.0424
	Horizontal=10	30.5587	0.9451	0.0474
	Horizontal=15	27.1622	0.9266	0.049
	Horizontal=20	25.9693	0.9119	0.0646
QSLST	Horizontal=5	29.5827	0.9545	0.0471
	Horizontal=10	28.3513	0.9097	0.0593
	Horizontal=15	23.7016	0.8815	0.0747
	Horizontal=20	26.1291	0.913	0.0597

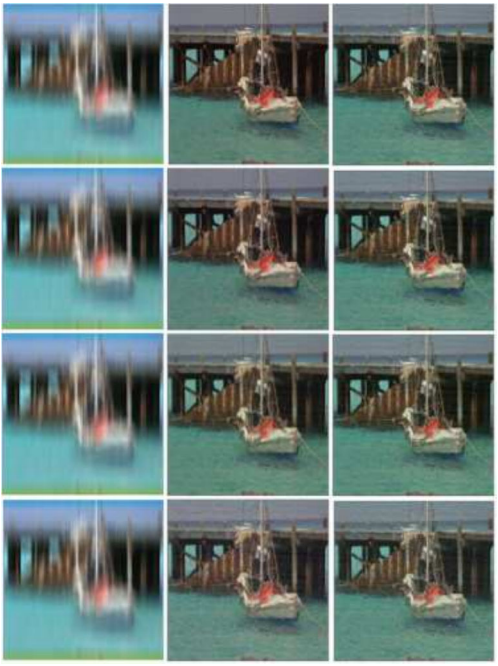

Fig. 6 The blurred and noisy images with SNR=35,30,25,20 (left column) and their restored results(From left to right are the blurred noisy image, the restored image by AQSLST, and the restored image by QSLST)

motion blur and noise more effectively than the standard QSLST method, as well as the aspects of deblurring and denoising of noisy images at different noise levels.

The numerical results of Fig. 6 are shown in Table 6 as follows. In Table 6, the performances of the two methods, AQSLST and QSLST, have their own characteristics. The AQSLST method has significant advantages in signal retention and processing effect. Its PSNR and SSIM are higher than those of QSLST under all SNR conditions, indicating that it can better retain the characteristic information of the signal. For example, when SNR=35, the PSNR of AQSLST is 33.6026 and the SSIM is 0.9922, while the

Table 6 The PSNR, SSIM and RE of the restored images

Method	Parameter	PSNR	SSIM	RE
AQSLST	SNR=35	33.6026	0.9922	0.018
	SNR=30	30.8356	0.98	0.0287
	SNR=25	27.2683	0.9316	0.0799
	SNR=20	22.8251	0.8312	0.148
QSLST	SNR=35	26.9079	0.9467	0.0784
	SNR=30	26.5206	0.9453	0.0804
	SNR=25	26.1619	0.9288	0.0903
	SNR=20	22.7158	0.8144	0.1447

PSNR of QSLST is only 26.9079 and the SSIM is 0.9467. This indicates that AQSLST can process signals more effectively under a high signal-to-noise ratio. Meanwhile, under the condition of a low signal-to-noise ratio, the performance degradation trend of AQSLST is relatively small, showing stronger robustness. Therefore, AQSLST is significantly superior to QSLST in the comprehensive performance of signal processing, especially in scenarios with high signal-to-noise ratios and high requirements for signal retention, where the advantages of AQSLST are more prominent.

8 Conclusion

In terms of image restoration, the QSLST method has demonstrated outstanding performance, especially excelling in image detail restoration and overall quality improvement. It can effectively reduce the errors in the restoration process and make the image closer to the original state. Under different degrees of ambiguity, the QSLST method still maintains a good recovery effect, showing strong robustness and adaptability. Meanwhile, during the image restoration process of the QSLST method, even in the face of a certain degree of noise interference, it can stably remove the noise, maintain the clarity and naturalness of the image, and provide reliable restoration effects for the complex image environment in practical applications.

The AQSLST method, as an adaptive version of the QSLST method, has further improved the performance in the image restoration task. The AQSLST method, through an adaptive parameter adjustment mechanism, can dynamically optimize the restoration process according to the characteristics of the image and the restoration requirements. This mechanism enables the AQSLST method to automatically adjust parameters when dealing with different degrees of blurriness, so as to better adapt to the complex image environment. The AQSLST method has significant advantages in maintaining image clarity and structural integrity. Meanwhile, it can effectively reduce relative errors and improve the quality of restored images. In terms of denoising, the AQSLST method, with its adaptive characteristics, can automatically adjust the denoising intensity according to the noise level in the image. It not only avoids the loss of details caused by excessive denoising, but also effectively suppresses noise in a high-noise environment, improving the visual quality of the image.

As summarized, the QSLST method provides a reliable image restoration solution with good robustness and adaptability. The AQSLST method, through its adaptive characteristics, not only has stronger adaptability and robustness in terms of image quality and structural integrity, but also can intelligently balance the relationship between denoising and detail retention, bringing higher quality, clearer and more natural restoration effects to the image restoration task.

Despite the achievements of QSLST and AQSLST methods in image recovery, there are still some limitations and areas that need further research. For example, the computational complexity of these methods is still relatively high, which may limit their application in real-time image processing scenarios. Furthermore, despite the significant improvements in adaptability and robustness, the AQSLST method still faces challenges when dealing with extreme cases of image degradation such as severe blurring or highly complex noise patterns.

Future work could focus on optimizing the computational efficiency of these methods to make them more suitable for real-time applications. In addition, exploring advanced techniques to enhance the ability of the method to handle more extreme and diverse image degradation conditions may be another direction for future research.

Author Contributions W.F. writes papers and conducts experiments, M.S. is responsible for extending the experimental ideas, and the supervisor is J.T. Make corrections and modifications.

Funding The work is supported by the National Natural Science Foundation of China (No. 12371378).

Data Availability No datasets were generated or analysed during the current study.

Declarations

Competing Interests The authors declare no competing interests.

Ethical Approval and Consent to participate Not applicable.

Consent for Publication Not applicable.

Human and Animal Ethics Not applicable.

References

1. Abubakar, J., Kumam, P., Garba, A.I., Ibrahim, A.H., Jirakitpuwapat, W.: Hybrid iterative scheme for variational inequality problem involving pseudo-monotone operator with application in signal recovery. Bulletin of the Iranian Mathematical Society **48**(6), 2995–3017 (2022)
2. Ben-Israel, A., Greville, T.N.E.: Generalized Inverses: Theory and Applications. s.n. (1974)
3. Bouhamidi, A., Enkhbat, R., Jbilou, K.: Conditional gradient tikhonov method for a convex optimization problem in image restoration. J. Comput. Appl. Math. **255**, 580–592 (2014)
4. Bouhamidi, A., Jbilou, K.: Sylvester tikhonov-regularization methods in image restoration. J. Comput. Appl. Math. **206**(1), 86–98 (2007)
5. Chen, Y.J., Pock, T.: Trainable nonlinear reaction diffusion: a flexible framework for fast and effective image restoration. IEEE Trans. Pattern Anal. Mach. Intell. **39**(6), 1256–1272 (2017)
6. Ding, W., Li, Y., Wang, D.: Special least squares solutions of the reduced biquaternion matrix equation AX = B with applications. Comput. Appl. Math. **40**(8), 279 (2021)
7. Dou, W., Li, Z., Tao, S., Feng, Q., Liu, H., Peng, Y., Zhang, X., Yu, M., Tai, X., Du, H.: Integrating RGB image with transformer for coded aperture snapshot spectral imaging restoration. Optics Communications **583**, 131642 (2025)
8. Duan, S.Q., Wang, Q.W.: A fast projected gradient algorithm for quaternion hermitian eigenvalue problems. Mathematics **13**(6), 994 (2025)
9. Fletcher, R.: Conjugate gradient methods for indefinite systems. Lect. Notes Math. **506**(1), 73–89 (1976)
10. Fong, D.C.L., Saunders, M.: Lsmr: An iterative algorithm for sparse least-squares problems. SIAM J. Sci. Comput. **33**(5), 2950–2971 (2011)
11. Garber, T., Tirer, T.: Image restoration by denoising diffusion models with iteratively preconditioned guidance. In: 2024 IEEE/CVF Conference on Computer Vision and Pattern Recognition (CVPR) (2024)
12. Golub, G.H., Heath, M.T., Wahba, G.: Generalized cross validation as a method for choosing a good ridge parameter. Technometrics **21**(2), 215–223 (1979)
13. Jia, Z.G., Jin, Q.Y., Ng, M.K., Zhao, X.L.: Non-local robust quaternion matrix completion for large-scale color image and video inpainting. IEEE Trans. Image Process. **31**, 3868–3883 (2022)

14. Jia, Z.G., Ng, M.K.: Robust quaternion matrix completion with applications to image inpainting. Numerical Linear Algebra with Applications **26**(4), e2245 (2019)
15. Jirakitpuwapat, W., Sombut, K., Yodjai, P., Seangwattana, T.: Enhancing image inpainting with deep learning segmentation and exemplar-based inpainting. Mathematical Methods in the Applied Sciences **48**(1), 1–15 (2025)
16. Kyung, S.G., Won, J.J., Pak, S.Y., Kim, S.W., Lee, S.Y., Park, K.G., Hong, G.S., Kim, N.K.: Generative adversarial network with robust discriminator through multi-task learning for low-dose ct denoising. IEEE Trans. Med. Imaging **44**(1), 499–518 (2025)
17. Lee, E., Hwang, Y.: Decomformer: Decompose self-attention of transformer for efficient image restoration. IEEE Access **12**, 38672–38684 (2024)
18. Li, T., Wang, Q.W.: Structure preserving quaternion biconjugate gradient method. SIAM J. Matrix Anal. Appl. **45**(1), 306–326 (2024)
19. Liang, H., Zhang, J., Wei, D., Zhu, J.: Hybrid regularization inspired by total variation and deep denoiser prior for image restoration. Complex & Intelligent Systems **10**(4), 4731–4739 (2024)
20. Ono, S.: Primal-dual plug-and-play image restoration. IEEE Signal Process. Lett. **24**(8), 1 (2017)
21. Paige, C.C., Saunders, M.A.: Algorithm 583: Lsqr: Sparse linear equations and least squares problems. ACM Transactions on Mathematical Software (TOMS) **8**(2), 195–209 (1982)
22. Paige, C.C., Saunders, M.A.: Lsqr: An algorithm for sparse linear equations and sparse least squares. ACM Transactions on Mathematical Software (TOMS) **8**(1), 43–71 (1982)
23. Saad, Y., Schultz, M.H.: Gmres: A generalized minimal residual algorithm for solving nonsymmetric linear systems. SIAM J. Sci. Comput. **7**(3), 856–869 (1986)
24. Shojaei-Fard, A., Amroudi, A.N.: An efficient method for solving a quaternionic least-squares problem. International Journal of Applied and Computational Mathematics **4**(1), 48 (2018)
25. Tibshirani, R.: Regression shrinkage and selection via the lasso. Journal of the Royal Statistical Society. Series B: Methodological **58**(1), 267–288 (1996)
26. Wang, R.C.: Functional Analysis and Optimization Theory. Beijing University of Aeronautics and Astronautics Press, Beijing (2003)
27. Wang, W.L., Qu, G.R., Song, C.Q., Ge, Y.R., Liu, Y.H.: Tikhonov regularization with conjugate gradient least squares method for large-scale discrete ill-posed problem in image restoration. Appl. Numer. Math. **204**, 147–161 (2024)
28. Wei, M.S.: Quaternion Matrix Computations. Nova Science Publishers, U.S.A. (2018)
29. Xie, L.M., Wang, Q.W., He, Z.H.: The generalized hand-eye calibration matrix equation $ax - yb = c$ over dual quaternions. Computational & Applied Mathematics **44**(1), 137 (2025)
30. Xu, H., Huang, T.Z., Lv, X.G., Liu, J.: The implementation of lsmr in image deblurring. Applied Mathematics & Information Sciences **8**(6), 3041–3048 (2014)
31. Xu, J., Fan, Y., You, S., et al.: Image denoising based on deep image prior combined sparsity with regularization by denoising. Circuits Syst Signal Process (2025). SN - 1531-5878
32. Xu, S., Zhang, J., Bo, L.L., Li, H.R., Zhang, H., Zhong, Z.M., Yuan, D.Q.: Singular vector sparse reconstruction for image compression. Computers & Electrical Engineering **91**, 107069 (2021)
33. Yang, Z., Diao, C., Li, B.: A robust hybrid deep learning model for spatiotemporal image fusion. Remote Sensing **13**(24), 5005 (2021)
34. Yodjai, P., Kumam, P., Kitkuan, D., Jirakitpuwapat, W., Plubtieng, S.: The halpern approximation of three operators splitting method for convex minimization problems with an application to image inpainting. Bangmod International Journal of Mathematical and Computational Science **5**, 58–75 (2019)
35. Yodjai, P., Kumam, P., Martínez-Moreno, J., Jirakitpuwapat, W.: Image inpainting via modified exemplar-based inpainting with two-stage structure tensor and image sparse representation. Mathematical Methods in the Applied Sciences **47**(11), 9027–9045 (2024)
36. Yuan, S.F., Wang, Q.W., Duan, X.F.: On solutions of the quaternion matrix equation and their applications in color image restoration. Applied Mathematics & Computation **221**, 10–20 (2013)
37. Zhang, F.X., Wei, M.S., Li, Y., Zhao, J.L.: Special least squares solutions of the quaternion matrix equation [formula omitted] with applications. Applied Mathematics & Computation **270**, 425–433 (2015)
38. Zhang, H.C., Xie, H.Z., Yao, H.X.: Blur-aware spatio-temporal sparse transformer for video deblurring. In: 2024 IEEE/CVF Conference on Computer Vision and Pattern Recognition (CVPR) (2024)

39. Zhang, Y.L., Zheng, P.Y., Yan, W.Q., Fang, C.Y., Cheng, S.S.: A unified framework for microscopy defocus deblur with multi-pyramid transformer and contrastive learning. In: 2024 IEEE/CVF Conference on Computer Vision and Pattern Recognition (CVPR) (2024)
40. Zhong, X., Chen, W., Guo, Z., Zhang, J., Luo, H.: Image inpainting using diffusion models to restore eaves tile patterns in Chinese heritage buildings. Autom. Constr. **171**, 105997 (2025)
41. Zhou, S.H., Chen, D.S., Pan, J.S., Shi, J.L., Yang, J.F.: Adapt or perish: Adaptive sparse transformer with attentive feature refinement for image restoration. In: 2024 IEEE/CVF Conference on Computer Vision and Pattern Recognition (CVPR) (2024)